Phase control of light amplification in steady and transient processes in an inverted-Y atomic system with spontaneously generated coherence

2014 Chinese Phys. B 23 044205

(http://iopscience.iop.org/1674-1056/23/4/044205)

Phase control of light amplification in steady and transient processes in an inverted-Y atomic system with spontaneously generated coherence*

Tian Si-Cong(田思聪)[a], Tong Cun-Zhu(佟存柱)[a], Wan Ren-Gang(万仁刚)[c], Ning Yong-Qiang(宁永强)[a], Qin Li(秦 丽)[a], Liu Yun(刘 云)[a], Wang Li-Jun(王立军)[a], Zhang Hang(张 航)[a], Wang Zeng-Bin(王增斌)[d], and Gao Jin-Yue(高锦岳)[b]†

[a] *State Key Laboratory of Luminescence and Application, Changchun Institute of Optics, Fine Mechanics and Physics, Chinese Academy of Sciences, Changchun* 130033, *China*

[b] *State Key Laboratory of Coherent Light and Atomic and Molecular Spectroscopy of Ministry of Education, College of Physics, Jilin University, Changchun* 130012, *China*

[c] *State Key Laboratory of Transient Optics and Photonics, Xi'an Institute of Optics and Precision Mechanics, Chinese Academy of Sciences, Xi'an* 710119, *China*

[d] *Quantum Engineering Center, Beijng Institute of Control Devices, Beijing* 100854, *China*

(Received 5 August 2013; revised manuscript received 16 September 2013; published online 10 February 2014)

We investigate the effects of spontaneously generated coherence (SGC) on both the steady and transient gain properties in a four-level inverted-Y-type atomic system in the presence of a weak probe, two strong coherent fields, and an incoherent pump. For the steady process, we find that the inversionless gain mainly origins from SGC. In particular, we can modulate the inversionless gain by changing the relative phase between the two fields. Moreover, the amplitude of the gain peak can be enhanced and the additional gain peak can appear by changing the detuning of the coupling field. As for the transient process, the transient gain properties can also be dramatically affected by the SGC. Compared to the case without SGC, the transient gain can be greatly enhanced with completely eliminated transient absorption by choosing the proper relative phase between the two fields. And the inverted-Y-type system with SGC can be simulated in both atomic and semiconductor quantum well systems avoiding the conditions of SGC.

Keywords: spontaneously generated coherence, gain without inversion, transient evolution, relative phase

PACS: 42.50.Gy, 42.50.Hz, 78.67.De **DOI:** 10.1088/1674-1056/23/4/044205

1. Introduction

As is well known, strong coherent fields can lead to a kind of coherence, the dynamically induced coherence (DIC), which is related to lasing without inversion (LWI) as well as many other optical phenomena in quantum optics. In the past decade, it has been shown that the LWI can provide us with an important and interesting alternative in cases where it is difficult or even impossible to create the required population inversion for conventional laser by incoherent pumping. The origin of the inversionless gain can be attributed to either inversion between dressed states or coherence among these states.[1,2] This kind of coherent condition can also be generated by tunnel-coupling two levels to the same continuum.[3] The relation between the steady state and the transient regime of LWI has been studied by Harris and Macklin[4] in a V-type three-level atom and a variety of schemes have been studied experimentally to realize the LWI.[5–8] Most recently, an observation of cw LWI in a gas of hot rubidium atoms in an optical cavity has been reported.[9] In Ref. [10], the authors demonstrated that LWI can be observed in the transient regime and Scully[11] has shown that it is possible to break detailed balance via quantum coherence, as in the case of LWI and the photo-Carnot quantum heat engine.[11] There is also application of quantum interference controlled resonance profiles from LWI to photodetection.[12] Also in specially designed semiconductor quantum well structures, Frogley *et al*.[13] have reported on the first observation of LWI.

On the other hand, it is also possible to obtain LWI through spontaneous emission in certain media if relevant decay pathways are correlated via the same vacuum modes, which is usually defined as spontaneously generated coherence (SGC).[14] The SGC can lead to a variety of novel quantum effects, such as the narrowing and quenching of spontaneous emission,[15–17] transparency of a short laser pulse,[18] and steady-state entanglement.[19] Apart from the interest of fundamentals, the SGC can also be found to have applications in many fields such as quantum information and computation,[20] all-optical switching,[21] and high-precision metrology.[22]

Moreover, it has been shown that the properties of an

*Project supported by the National Basic Research Program of China (Grant Nos. 2011CB921603 and 2013CB933300), the National Natural Science Foundation of China (Grant Nos. 11304308, 61076064, and 61176046), Natural Science Foundation of Jilin Province, China (Grant Nos. 20140101203JC), and the Hundred Talents Program of the Chinese Academy of Sciences.

†Corresponding author. E-mail: jygao@mail.jlu.edu.cn

atomic system with SGC are sensitive to the relative phase of the applied field. The investigations of the effects of SGC and the relative phase are mostly related to three-level atomic systems,[23–26] which have been used to obtain LWI.[27,28] And there are other papers considering a more complex atomic system — the four-level atomic system with the effects of SGC and the relative phase.[29–33] On the other hand, most of these studies related to SGC focused on the steady-state response of the medium. There are only a few studies of the effect of SGC on the transient gain properties.[34–36] Since the transient properties are very important for its potential application in an optical switch, which is an important technique in quantum computing and quantum information,[37] the SGC on transient gain properties must be addressed.

Recently, a four-level inverted-Y atomic system has been extensively investigated to suppress two-photon absorption,[38] obtain EIT,[39] realize two-channel quantum memory,[40] operatethe quantum gate,[41] generate nonclassical paired photons,[42] and the enhancement of cross-Kerr effect.[43] But there is no work studying the effects of SGC and the relative phase on the gain properties in such a system. In the present paper, we investigate the phase control of light amplification without inversion in a four-level inverted-Y-type system with SGC in both the steady and transient processes. Due to the effect of SGC, the steady and transient gains are quite different from that of a conventional inverted-Y-type system without SGC. Especially, the steady-state inversionless gain can be enhanced due to the SGC effect. By changing the relative phase between the coupling and probe fields, the gain profile and the gain amplitude can be modulated. Moreover we can obtain a much larger gain and an additional gain peak by changing the detuning of the coupling field, which cannot be obtained in a three-level Λ atomic system.[27] Also the transient gain can be greatly enhanced, and the transient absorption can be completely eliminated just by choosing the proper relative phase between the coupling and probe fields.

Note that the SGC only exists in such atoms having closely-lying levels and that corresponding dipole matrix elements are not orthogonal.[44] However, these rigorous conditions are rarely met in real atoms. The experiment on spontaneous emission from sodium dimers was conducted a few years ago.[45] However, another experiment[46] on a similar system failed to reproduce the same results. Fortunately, the type of quantum interference resulting from the incoherent decay processes can be simulated with atoms in the dressed-state picture.[47,48] Most recently, we have observed the SGC on absorption and fluorescence in rubidium atomic beam via the coherent laser field experimentally.[49,50] On the other hand, quantum wells (QWs), which can be viewed as the two-dimensional electron gas, have properties similar to that of atomic vapor such as the discrete energy levels. By choosing the materials and structure dimensions in device design, their transition energies, dipole moments, and symmetries can be engineered as desired.[51–54] So before the end of this paper, we give two examples of possible experimental observations of the features in both the atomic system and the QWs system.

The rest of this paper is organized as follows. In Section 2, we introduce a four-level inverted-Y-type system and obtain the corresponding density-matrix equations. In Section 3, we investigate the dependence of the steady gain property on the relative phase between the probe and the coherent field. In Section 4, we investigate the dependence of the transient gain property on the relative phase between the probe and the coherent field. In Section 5, we discuss a possible experiment to attain the four-level inverted-Y-type system with SGC. Finally, in Section 6, we draw a brief conclusion.

2. System and the corresponding density-matrix equations

A four-level inverted-Y-type atomic system is shown in Fig. 1(a). Level $|1\rangle$ and level $|4\rangle$ are two closely-lying lower levels. A coupling field with frequency ω_1 and Rabi frequency $\Omega_1 = \boldsymbol{\mu}_{23} \cdot \boldsymbol{\varepsilon}_1 / 2\hbar$ drives the transition $|3\rangle \leftrightarrow |2\rangle$. Another coupling field with frequency ω_2 and Rabi frequency $\Omega_2 = \boldsymbol{\mu}_{42} \cdot \boldsymbol{\varepsilon}_2 / 2\hbar$ drives the transition $|2\rangle \leftrightarrow |4\rangle$. A weak probe field with frequency ω_p and Rabi frequency $\Omega_\mathrm{p} = \boldsymbol{\mu}_{12} \cdot \boldsymbol{\varepsilon}_\mathrm{p} / 2\hbar$ is applied to the transition $|2\rangle \leftrightarrow |1\rangle$, which is also pumped with a rate Λ by an incoherent field. The $\Delta_1 = \omega_{32} - \omega_1$, $\Delta_2 = \omega_{24} - \omega_2$, and $\Delta_\mathrm{p} = \omega_{21} - \omega_\mathrm{p}$ are detunings of the corresponding fields. The γ_3, γ_{24}, and γ_{21} are the spontaneous emission rates from level $|3\rangle$ to level $|2\rangle$, level $|2\rangle$ to level $|4\rangle$, and level $|2\rangle$ to level $|1\rangle$, respectively.

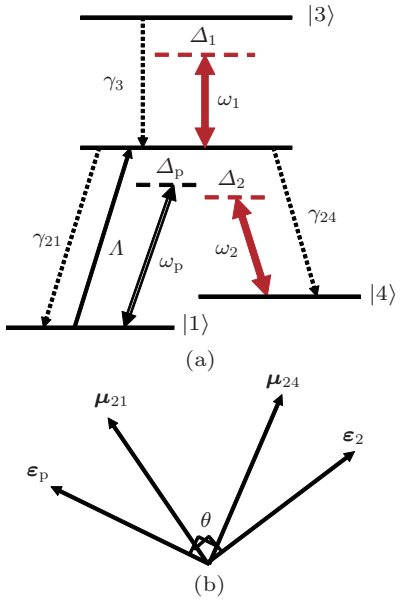

Fig. 1. (color online) (a) Schematic diagram of an inverted-Y-type atomic system. (b) The field polarizations are chosen so that one field drives only one transition.

In the interaction picture, the semiclassical Hamiltonian of this system in the rotating wave approximation and the dipole approximation can be written as

$$\begin{aligned} H_{\rm I} &= \Delta_{\rm p}|2\rangle\langle 2| + (\Delta_{\rm p}+\Delta_1)|3\rangle\langle 3| \\ &\quad + (\Delta_{\rm p}-\Delta_2)|4\rangle\langle 4| + [\Omega_{\rm p}(|1\rangle\langle 2| \\ &\quad + |2\rangle\langle 1|) + \Omega_1(|2\rangle\langle 3| + |3\rangle\langle 2|) \\ &\quad + \Omega_2(|4\rangle\langle 2| + |2\rangle\langle 4|) + \text{H.c.}]. \end{aligned} \tag{1}$$

The density-matrix equations of motion can be derived as follows:

$$\begin{aligned} \dot{\sigma}_{12} &= \left(\mathrm{i}\Delta_{\rm p} - \frac{\gamma_{21}+\gamma_{24}+\Lambda}{2}\right)\sigma_{12} \\ &\quad + \mathrm{i}\Omega_{\rm p}^*(\sigma_{22}-\sigma_{11}) - \mathrm{i}\Omega_1\sigma_{13} - \mathrm{i}\Omega_2^*\sigma_{14}, \end{aligned} \tag{2a}$$

$$\begin{aligned} \dot{\sigma}_{13} &= \left[\mathrm{i}(\Delta_{\rm p}+\Delta_1) - \frac{\Lambda+\gamma_3}{2}\right]\sigma_{13} \\ &\quad + \mathrm{i}\Omega_{\rm p}^*\sigma_{23} - \mathrm{i}\Omega_1^*\sigma_{12}, \end{aligned} \tag{2b}$$

$$\begin{aligned} \dot{\sigma}_{14} &= \left[\mathrm{i}(\Delta_{\rm p}-\Delta_2) - \frac{\Lambda}{2}\right]\sigma_{14} + \mathrm{i}\Omega_{\rm p}^*\sigma_{24} \\ &\quad - \mathrm{i}\Omega_2\sigma_{12} + \eta\sqrt{\gamma_{21}\gamma_{24}}\cos\theta\sigma_{22}, \end{aligned} \tag{2c}$$

$$\begin{aligned} \dot{\sigma}_{22} &= (\mathrm{i}\Omega_{\rm p}\sigma_{12} - \mathrm{i}\Omega_{\rm p}^*\sigma_{21}) + (\mathrm{i}\Omega_1^*\sigma_{32} - \mathrm{i}\Omega_1\sigma_{23}) \\ &\quad + (\mathrm{i}\Omega_2\sigma_{42} - \mathrm{i}\Omega_2^*\sigma_{24}) + \Lambda\sigma_{11} \\ &\quad + \gamma_3\sigma_{33} - (\gamma_{21}+\gamma_{24})\sigma_{22}, \end{aligned} \tag{2d}$$

$$\begin{aligned} \dot{\sigma}_{23} &= \left[\mathrm{i}\Delta_1 - \frac{\gamma_{21}+\gamma_{24}+\gamma_3}{2}\right]\sigma_{23} \\ &\quad + \mathrm{i}\Omega_1^*(\sigma_{33}-\sigma_{22}) + \mathrm{i}\Omega_{\rm p}\sigma_{13} + \mathrm{i}\Omega_2\sigma_{43}, \end{aligned} \tag{2e}$$

$$\begin{aligned} \dot{\sigma}_{24} &= -\left(\mathrm{i}\Delta_2 + \frac{\gamma_{21}+\gamma_{24}}{2}\right)\sigma_{24} \\ &\quad + \mathrm{i}\Omega_2(\sigma_{44}-\sigma_{22}) + \mathrm{i}\Omega_{\rm p}\sigma_{14} + \mathrm{i}\Omega_1^*\sigma_{34}, \end{aligned} \tag{2f}$$

$$\dot{\sigma}_{33} = \mathrm{i}\Omega_1\sigma_{23} - \mathrm{i}\Omega_1^*\sigma_{32} - \gamma_3\sigma_{33}, \tag{2g}$$

$$\dot{\sigma}_{34} = -\left[\mathrm{i}(\Delta_1+\Delta_2) + \frac{\gamma_3}{2}\right]\sigma_{34} + \mathrm{i}\Omega_1\sigma_{24} - \mathrm{i}\Omega_2\sigma_{32}, \tag{2h}$$

$$\dot{\sigma}_{44} = \mathrm{i}\Omega_2^*\sigma_{24} - \mathrm{i}\Omega_2\sigma_{42} + \gamma_{24}\sigma_{22}. \tag{2i}$$

The above equations are constrained by $\sigma_{ij} = \sigma_{ji}^*$ and $\sigma_{11}+\sigma_{22}+\sigma_{33}+\sigma_{44} = 1$. The term $\eta\sqrt{\gamma_{21}\gamma_{24}}\cos\theta$ represents the quantum interference effect resulting from the cross coupling between spontaneous emissions $|2\rangle \to |4\rangle$ and $|2\rangle \to |1\rangle$, known as the SGC effect. If levels $|1\rangle$ and $|4\rangle$ lie so close that the SGC effect must be taken into account, then $\eta = 1$, otherwise $\eta = 0$. θ is the angle between the dipole matrix elements $\boldsymbol{\mu}_{12}$ and $\boldsymbol{\mu}_{42}$. If the matrix elements $\boldsymbol{\mu}_{12}$ and $\boldsymbol{\mu}_{42}$ are orthogonal to each other, the SGC disappears. So the existence of the SGC depends on the nonorthogonality of the matrix elements $\boldsymbol{\mu}_{12}$ and $\boldsymbol{\mu}_{42}$. We arrange fields $\omega_{\rm p}$ and ω_2 as in Fig. 1(b), so that one field acts on only one transition. To obtain the remarkable SGC effect on optical properties of the system we assume that the ground levels are nearly degenerate, as for large energy spacing, the rapid oscillations in σ_{41} will average out any such effects.[23] In the case of a weak probe field, the incoherent pump plays a very important role in reserving the SGC effect. Because without the incoherent pump, the probe field is so weak that all the population is reserved in the ground state, thus the spontaneous emission does not take place, nor does the SGC effect.

The existence of the SGC effect makes the system quite sensitive to phases of the probe and the coupling field, so the Rabi frequencies must be treated as complex parameters. Thus we write the Rabi frequencies $\Omega_{\rm p}$, Ω_1, and Ω_2, as the forms: $\Omega_{\rm p} = G_{\rm p}\mathrm{e}^{-\mathrm{i}\Phi_{\rm p}}$, $\Omega_1 = G_1$, and $\Omega_2 = G_2\mathrm{e}^{-\mathrm{i}\Phi_2}$, where $\Phi_{\rm p}$ and Φ_2 denote phases of the probe field $\omega_{\rm p}$ and the coupling field ω_2, respectively. Assume that the Rabi frequency Ω_1 is a real parameter throughout the paper, then we will be able to write $\rho_{21} = \sigma_{21}\mathrm{e}^{\mathrm{i}\Phi_{\rm p}}$, $\rho_{24} = \sigma_{24}\mathrm{e}^{\mathrm{i}\Phi_2}$, $\rho_{31} = \sigma_{31}\mathrm{e}^{\mathrm{i}\Phi_{\rm p}}$, $\rho_{34} = \sigma_{34}\mathrm{e}^{\mathrm{i}\Phi_2}$, $\rho_{41} = \sigma_{41}\mathrm{e}^{\mathrm{i}\Phi}$, and $\rho_{ij} = \sigma_{ij}$, where $\Phi = \Phi_{\rm p} - \Phi_2$. Therefore we obtain equations about ρ_{ij} $(i,j = 1,2,3,4)$ which are found to be identical with Eq. (2) except that η is replaced by $\eta\mathrm{e}^{\mathrm{i}\Phi}$, $\Omega_{\rm p}$, Ω_1, and Ω_2 are replaced by $G_{\rm p}$, G_1, and G_2, respectively, where $G_{\rm p}$, G_1, and G_2 are treated as real parameters.

As is well known, in the limit of a weak probe, the gain absorption coefficient for the probe laser on transition $|2\rangle \to |1\rangle$ is proportional to the imaginary part of ρ_{12}, which can be obtained from Eq. (2). If $\mathrm{Im}(\rho_{12}) > 0$, the probe laser will be amplified. The complicated analytical solutions of Eq. (2) involving many parameters are almost impossible to show the physical information evidently, thus we shall investigate the dependence of steady-state absorption properties and transient absorption properties by numerical calculations of $\mathrm{Im}(\rho_{21})$ instead. Note that in this paper, parameters $G_{\rm p}$, G_1, G_2, $\Delta_{\rm p}$, Δ_1, Δ_2, Λ, γ_{24}, and γ_3 are scaled by γ_{21}.

3. Effects of SGC on the steady gain (absorption) properties

First we consider the effect of SGC on the steady gain properties. In Fig. 2, with $\Lambda = 0.5$, $\gamma_{21} = 1$, $\gamma_{24} = 2$, $\gamma_3 = 0.5$,

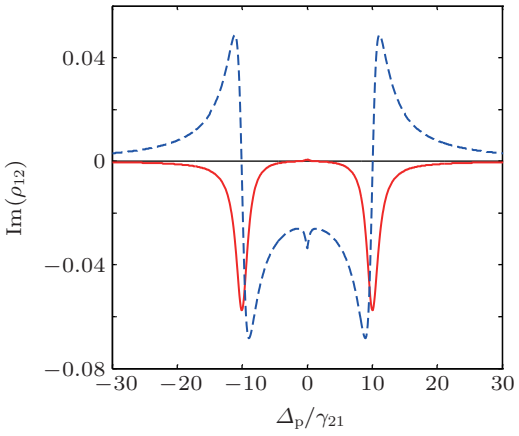

Fig. 2. (color online) Dependences of the probe gain $\mathrm{Im}(\rho_{12})$ on probe detuning $\Delta_{\rm p}/\gamma_{21}$ with $\theta = \pi/4$, $\Lambda = 0.5$, $\gamma_{21} = 1$, $\gamma_{24} = 2$, $\gamma_3 = 0.5$, $\Delta_1 = \Delta_2 = 0$, $G_{\rm p} = 0.01$, $G_1 = 10/\sqrt{2}$, and $G_2 = 10/\sqrt{2}$. The red solid curve is the case with $\eta = 0$, while the blue dashed curve is that with $\eta = 1$ and $\Phi = 0$.

$\theta = \pi/4$, $\Delta_1 = \Delta_2 = 0$, $G_\mathrm{p} = 0.01$, $G_1 = 10/\sqrt{2}$, and $G_2 = 10/\sqrt{2}$, we plot the steady-state probe gain $\mathrm{Im}(\rho_{12})$ against the probe detuning Δ_p. It is shown that when no SGC effect exists in this system ($\eta = 0$), the probe is amplified only around $\Delta_\mathrm{p} = 0$ with a very small amplitude (red solid curve). While in the case of considering the SGC effect ($\eta = 1$), the probe is amplified elsewhere with a much larger amplitude (blue dashed curve). This means that in the case of $\eta = 1$, the SGC contributes much more to the probe gain.

Now, we give the physical interpretations of the spectral features found in Fig. 2. When η is replaced by $\eta\,\mathrm{e}^{\mathrm{i}\Phi}$, Ω_p, Ω_1, and Ω_2 are replaced by G_p, G_1, and G_2, we can obtain equations about ρ_{ij} $(i,j = 1,2,3,4)$ which are found to be identical with Eq. (2). Then the steady-state solution of ρ_{12} can be written as

$$\rho_{12} = \frac{\mathrm{i}G_\mathrm{p}\tilde{\gamma}_{13}\tilde{\gamma}_{14}(\rho_{22}-\rho_{11}) - (G_\mathrm{p}G_1\tilde{\gamma}_{14}\rho_{23} + G_\mathrm{p}G_2\tilde{\gamma}_{13}\rho_{24}) + \mathrm{i}G_2\tilde{\gamma}_{13}\eta\cos\theta\sqrt{\gamma_{21}\gamma_{24}}\rho_{22}}{-\tilde{\gamma}_{12}\tilde{\gamma}_{13}\tilde{\gamma}_{14} - G_1^2\tilde{\gamma}_{14} - G_2^2\tilde{\gamma}_{13}}, \tag{3a}$$

where

$$\tilde{\gamma}_{12} = \mathrm{i}\Delta_\mathrm{p} - (\gamma_{21} + \gamma_{24} + \Lambda)/2, \tag{3b}$$

$$\tilde{\gamma}_{13} = \mathrm{i}(\Delta_\mathrm{p} + \Delta_1) - (\Lambda + \gamma_3)/2, \tag{3c}$$

$$\tilde{\gamma}_{14} = \mathrm{i}(\Delta_\mathrm{p} - \Delta_2) - \Lambda/2. \tag{3d}$$

From Eq. (3), we find that ρ_{12} is contributed by three terms: the population difference term (proportional to $\rho_{22} - \rho_{11}$), the DIC term (proportional to ρ_{23} and ρ_{24}), and the SGC term (proportional to $\eta\sqrt{\gamma_{21}\gamma_{24}}\cos\theta$). The contributions from these three terms to the probe gain without SGC ($\eta = 0$) and with SGC ($\eta = 1$) are numerically computed and shown in Fig. 3.

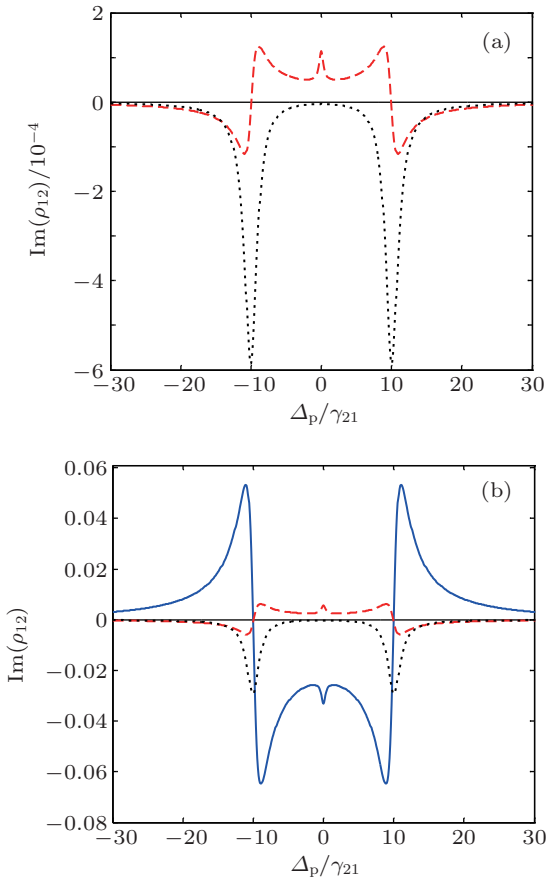

Fig. 3. (color online) Gain contributions from three terms. The population difference term, the DIC term, and the SGC term are plotted in a black dotted line, red dashed line, and blue solid line, respectively. (a) For considering no SGC effect ($\eta = 0$), the contribution from DIC terms is magnified 10 times. (b) For considering the SGC effect ($\eta = 1$), the contributions from the population difference term and DIC term are magnified 50 and 500 times, respectively. Other parameters are the same as those in Fig. 2.

When $\eta = 0$, from Fig. 3(a) we can find that $\rho_{22} - \rho_{11} < 0$, so there is no population inversion between level $|2\rangle$ and level $|1\rangle$. Thus the contribution to $\mathrm{Im}(\rho_{12})$ from the population inversion is always negative and the contribution from DIC term is positive in the region where the LWI is exhibited (the contributions from DIC are magnified 10 times). So the probe gain without the SGC effect is due to the DIC resulting from the coherent fields. In Fig. 3(b), we can see that when $\eta = 1$, the contribution from the DIC term and population difference term in the presence of SGC are the same as those in the absence of SGC. There is also no population inversion between level ρ_{22} and level ρ_{11} and the contribution from the SGC term exhibits a Mollow-like profile and its amplitude is much larger than those of the other two terms (the contributions from $\rho_{22} - \rho_{11}$ and DIC terms are magnified 50 and 500 times, respectively). We can also notice that the profile is almost the same as the probe gain profile plotted by the blue dashed curve in Fig. 2. From Fig. 3(b), we can conclude that the behavior of the probe gain mainly depends on the SGC term (proportional to $\eta\sqrt{\gamma_{21}\gamma_{24}}\cos\theta$). So in both situations, the probe gain is inversionless gain, and when $\eta = 0$, it originates from DIC, while when $\eta = 1$, it mainly derives from the SGC.

As is well known, the effect of quantum interference is very sensitive to the orientation of the atomic dipole polarization. When the angle θ between the dipole matrix elements $\boldsymbol{\mu}_{12}$ and $\boldsymbol{\mu}_{42}$ changes from 0 to $\pi/2$, the quantum interference of the atomic system changes from a maximal extent to nil. In Fig. 4(a), we plot the dependences of probe gain $\mathrm{Im}(\rho_{12})$ on probe detuning Δ_p and angle θ. The structures of the spectra are nearly the same for different values of parameter θ, but the amplitude of the probe gain for the small angle is greater than that for the large angle. For instance, we depict the probe gain

as a function of Δ_p under several fixed values of angle θ in Fig. 4(b). The enhancement of the gain can be due to the increased quantum interference when reducing the angle. Once again, we obtain the result that the probe gain mainly originates from the SGC effect, which can also be explained by the third part of Eq. (3).

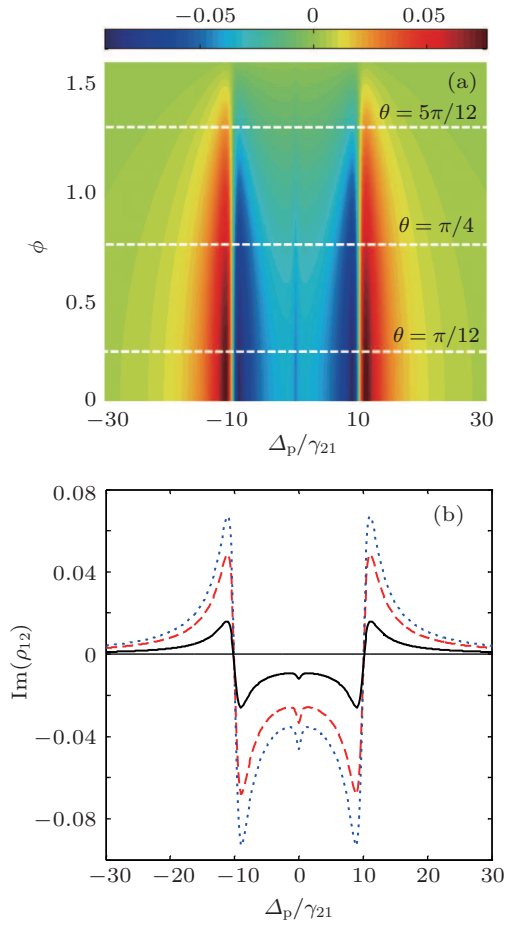

Fig. 4. (color online) (a) Dependences of the probe gain $\mathrm{Im}(\rho_{12})$ on probe detuning Δ_p/γ_{21} and angle θ with $\eta = 1$, $\Phi = 0$. (b) Dependences of the probe gain $\mathrm{Im}(\rho_{12})$ on probe detuning Δ_p/γ_{21} for fixed values of θ: $\theta = \pi/12$ (blue dotted line), $\pi/4$ (red dashed line), and $5\pi/12$ (black solid line). Other parameters are the same as those in Fig. 2.

To obtain a deeper insight into the modulation effect of the relative phase Φ on the probe gain of the system with SGC, we display the dependence of the probe gain $\mathrm{Im}(\rho_{12})$ as a function of detuning Δ_p and relative phase Φ in Fig. 5(a). It is shown that at different detunings, we obtain different modulation amplitudes of the probe gain, and the modulation period of the probe gain is always 2π. While for different values of Φ, the largest probe gains correspond to different detunings. For instance, we depict the probe gains each as a function of Δ_p under several fixed values of relative phase Φ in Fig. 5(b). When $\Phi = \pi/2$ and $\Phi = 3\pi/2$, a much larger probe gain can be achieved at $\Delta_p = \sqrt{G_1^2 + G_2^2} = G$ or $\Delta_p = -\sqrt{G_1^2 + G_2^2} = -G$, which corresponds to the eigenvalue of the dressed-state sublevel

$$|+\rangle = \frac{1}{\sqrt{2}}\left(\frac{G_1}{G}|2\rangle + \frac{G_2}{G}|3\rangle - |4\rangle\right)$$

or

$$|-\rangle = \frac{1}{\sqrt{2}}\left(\frac{G_1}{G}|2\rangle + \frac{G_2}{G}|3\rangle + |4\rangle\right)$$

of level $|2\rangle$ under the condition of $\Delta_1 = \Delta_2 = 0$. While $\Phi = \pi$, the probe signal with a smaller amplitude can be amplified in a much larger spectrum range: $\delta_{\omega_p} = 2G$, which is the energy spacing between the two dressed-state sublevels $|+\rangle$ and $|-\rangle$.

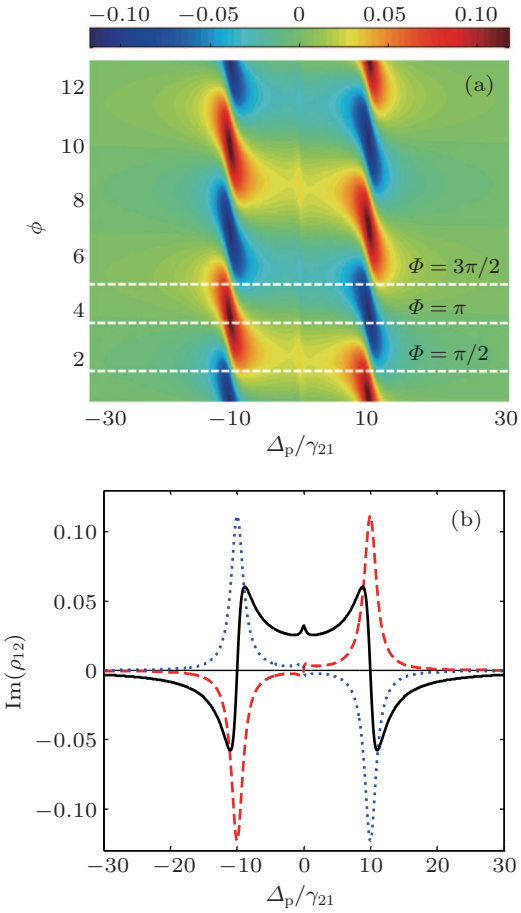

Fig. 5. (color online) (a) Dependences of the probe gain $\mathrm{Im}(\rho_{12})$ on probe detuning Δ_p/γ_{21} and relative phase Φ with $\eta = 1$ and $\theta = \pi/4$. (b) Dependences of the probe gain $\mathrm{Im}(\rho_{12})$ on probe detuning Δ_p/γ_{21} for fixed values of relative phase Φ: $\Phi = \pi/2$ (blue dotted line), π (black solid line), and $3\pi/2$ (red dashed line). Other parameters are the same as those in Fig. 2.

Last, we display in Fig. 6 the dependences of the probe gain $\mathrm{Im}(\rho_{12})$ each as a function of detuning Δ_p when the two coupling fields are not in resonance. The blue dashed line is for the case of $\Delta_1 + \Delta_2 = 0$, $(\Delta_1 \neq 0, \Delta_2 \neq 0)$, while the red solid line is for the case of $\Delta_1 + \Delta_2 \neq 0$. When $\Delta_1 + \Delta_2 = 0$, $(\Delta_1 \neq 0, \Delta_2 \neq 0)$, the results are similar to the previous results obtained from the atomic system.[27] While when $\Delta_1 + \Delta_2 = 0$ is not satisfied, the amplitude of the gain signal can be increased dramatically in the case of $\Phi = \pi/2$ as shown in Fig. 6(a) and the additional gain peak can be obtained in the middle in the case of $\Phi = 3\pi/2$ as shown in Fig. 6(b). So we

can obtain much larger probe gain or additional gain peak just by changing the additional coupling field ω_1 and these results cannot be obtained in the Λ atomic system with SGC.

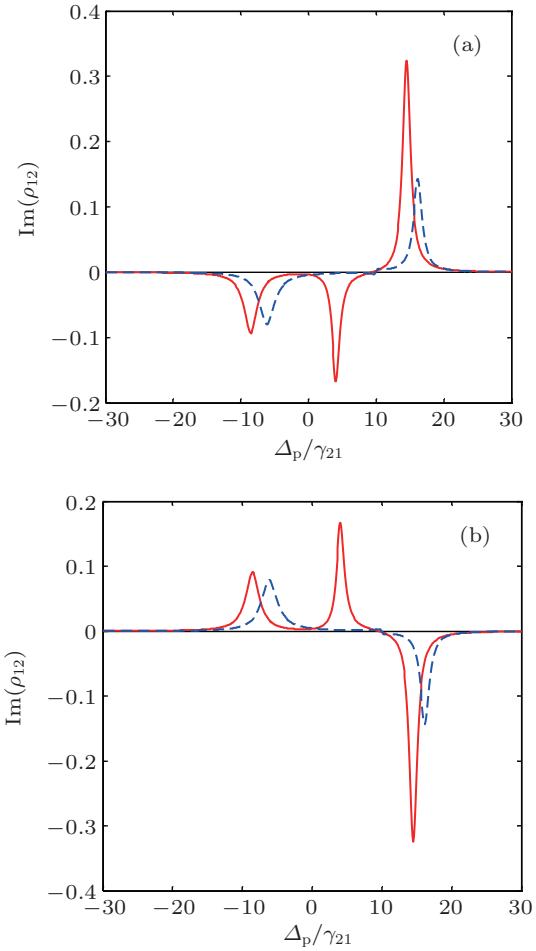

Fig. 6. (color online) Dependences of the probe gain $\mathrm{Im}(\rho_{12})$ on the probe detuning Δ_p/γ_{21} with $\eta = 1$ and different values of Δ_1 and Δ_2: $\Delta_1 = -10$, $\Delta_2 = 10$ (blue dashed line), $\Delta_1 = 0, \Delta_2 = 10$ (red solid line). (a) $\Phi = \pi/2$, (b) $\Phi = 3\pi/2$. Other parameters are the same as those in Fig. 2.

4. Effects of SGC on the transient gain (absorption) properties

Since the transient properties of EIT are very important for its potential application, the effect of SGC on transient properties must be addressed. Under the initial condition $\rho_{11} = \rho_{44} = 0.5$ and $\rho_{ij} = 0$ $(i, j = 1\text{–}4)$, we derive the time-dependent numerical solutions of Eq. (2) in the following. First, we consider the case where both coupling lasers and the probe laser are in resonance $(\Delta_1 = \Delta_2 = \Delta_p = 0)$. In Fig. 7, with different values of Φ and the same other parameters as those used in Fig. 2, we plot the time evolution of the gain–absorption coefficient $\mathrm{Im}(\sigma_{21})$ without considering the SGC effect $(\eta = 0)$ and with considering the SGC effect $(\eta = 1)$.

Figure 7(a) shows that when $\eta = 0$, the probe laser shows oscillatory behavior versus time, i.e., the probe laser exhibits periodic amplification and absorption. In Fig. 7(b) we show that the transient property is greatly changed when the SGC effect is included $(\eta = 1)$. Further the transient property exhibits different features with different values of relative phase Φ. With $\Phi = \pi$ (red dashed curve), the probe laser can always exhibit considerably large gain without any absorption in the whole process. The probe gain oscillates around the nonzero steady-state value and eventually reaches a positive steady-state value. On the contrary, with $\Phi = 0$ (blue dotted curve), the transient gain disappears, only leaving the transient absorption oscillation bellow the zero-absorption line and finally reaches a negative steady-state value. In these such two cases, by comparing to the case of $\eta = 0$, we can see that firstly, the probe laser does not exhibit periodic amplification nor absorption. Secondly, the amplitude of the oscillatory is much larger. Thirdly, the steady process gain (or absorption) can reach a larger value. Fourthly, the oscillatory frequency is reduced. Then for $\Phi = \pi/2, 3\pi/2$, the time evolutions of the gain–absorption coefficient $\mathrm{Im}(\sigma_{21})$ have the same structure (black solid line). For the sake of clarity, this result is magnified 10 times. We can see that the probe laser exhibits periodic amplification and absorption with the small amplitude of the oscillatory, which is similar to that for the case $\eta = 0$. To conclude, with the help of SGC, we can obtain a much larger transient gain just by choosing a proper value of relative phase Φ.

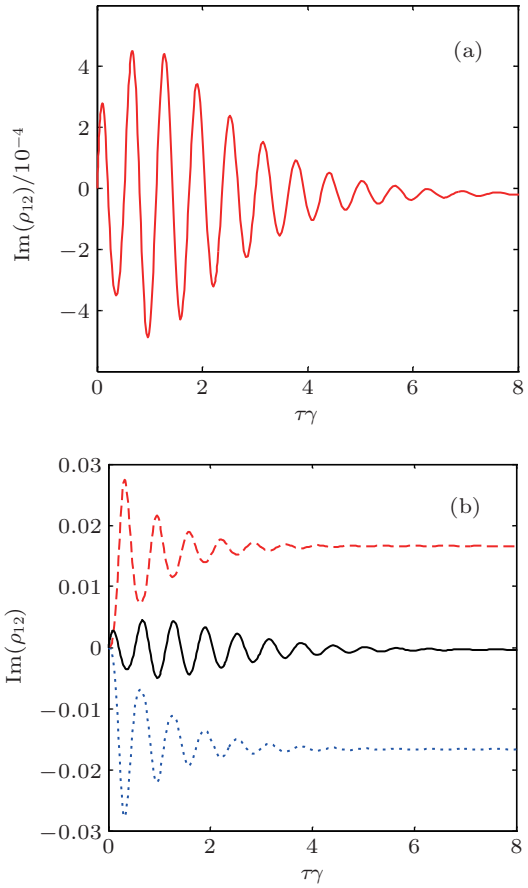

Fig. 7. (color online) Time evolutions of the gain–absorption coefficient $\mathrm{Im}(\rho_{12})$ for $\Delta_p = 0$ in the cases: (a) without considering the SGC effect $(\eta = 0)$, (b) with considering the SGC effect $(\eta = 1)$ and different values relative phase Φ: $\Phi = 0$ (blue dotted line), π (red dashed line), $\pi/2$, and $3\pi/2$ (black solid line, the result is magnified 10 times). Other parameters are the same as those in Fig. 2.

Then we fix the values of the relative phase and investigate the time evolutions of the gain-absorption coefficient $\mathrm{Im}(\sigma_{21})$ for different values of θ with considering the effect of SGC ($\eta = 1$). In Fig. 8, we set $\Phi = \pi$, and the other parameters are the same as those in Fig. 2. From the figure we can see that for different values of θ, the probe laser can always exhibit a considerably large gain without any absorption in the whole process and the oscillatory frequencies are the same. The only difference is that the smaller the value of θ, the larger the value of amplitude of the oscillatory and the steady-state gain value.

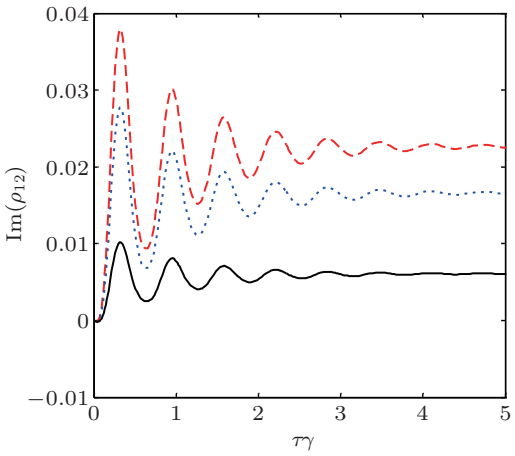

Fig. 8. (color online) Time evolutions of the gain–absorption coefficient $\mathrm{Im}(\rho_{12})$ with considering the SGC effect ($\eta = 1$) with $\Delta_p = 0$, $\Phi = \pi$ and different values of angle θ: $\theta = \pi/12$ (red dashed line), $\pi/4$ (blue dotted line), and $5\pi/12$ (black solid line). Other parameters are the same as those in Fig. 2.

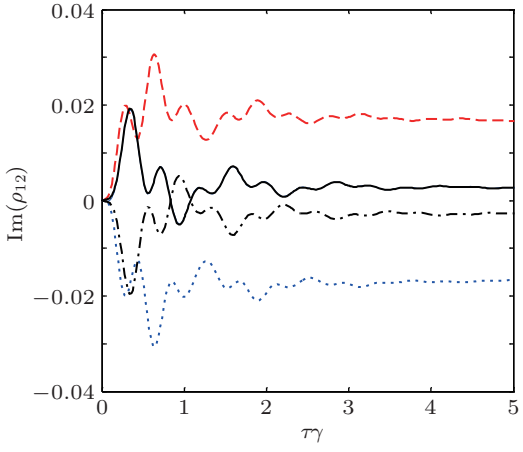

Fig. 9. (color online) Time evolutions of the gain–absorption coefficient $\mathrm{Im}(\rho_{12})$ with considering the SGC effect ($\eta = 1$) for $\Delta_p = 5$ and different values of relative phase Φ: $\Phi = 0$ (blue dotted line), $\pi/2$ (black dotted–dashed line), π (red dashed line), and $3\pi/2$ (black solid line). Other parameters are the same as those in Fig. 2.

Last, we consider the cases of the nonresonant probe laser and resonance coupling lasers ($\Delta_p = 5, \Delta_1 = \Delta_2 = 0$). In Fig. 9, with different values of relative phase Φ we plot the time evolutions of the gain–absorption coefficient $\mathrm{Im}(\sigma_{21})$ with considering the SGC effect. The other parameters are the same as the ones used in Fig. 2. When $\Phi = \pi/2$ (black dotted–dashed curve), both transient absorption and transient gain can be found in the transient process, and the transient absorption dominates over the transient gain. On the contrary, when $\Phi = 3\pi/2$ (black solid curve), both transient absorption and transient gain can also be found in the transient process, and the transient gain dominates over the transient absorption. In both cases the steady process can reach a very small value. When $\Phi = \pi$ (red dashed curve), the probe laser can always exhibit a considerably large gain without any absorption in the whole process. While, in the case of $\Phi = 0$ (blue dotted curve), the transient gain completely disappears, leaving only large transient absorption. From Fig. 9, we can conclude that it is similar to the resonant case that different values of relative phase Φ can also lead to different gain properties of the transient process.

5. Possible experiments

To observe the predicted phenomena associated with SGC, we need two closely separated levels with nonorthogonal dipole moments. It is worth noting that so far no real atoms or molecules have been found to exhibit observable SGC due to the rigorous conditions. Fortunately such a system can be attained in a four-level inverted-Y-type system without SGC, which is equivalent to the system with SGC in the dressed state representation of an additional field. The transition dipoles of the two dressed states to intermediate level would be parallel, which satisfies the specific arrangement for dipole moments and field polarizations in our system. Here we show two examples of possible experimental observations on the features predicted in this paper in both atomic and QW systems.

In the rubidium atoms, Wang *et al.*[49] have experimentally investigated the effects of SGC in a four-level inverted-Y-type system on the hyperfine levels of ^{85}Rb. Here we use the same energy-level scheme as that for ^{85}Rb, which is shown in Fig. 10(a). The two ground states $|1\rangle$ and $|4\rangle$ are presented by $5S_{1/2}$, $F = 3$ and $5S_{1/2}$, $F = 2$. The intermediate level $|2\rangle$ and upper level $|3\rangle$ are provided by $5P_{1/2}$, $F = 3$ and $5D_{3/2}$, $F = 4$. The probe field ω_p drives the $|1\rangle \leftrightarrow |2\rangle$ transition. The coupling fields ω_1 and ω_2 drive the $|2\rangle \leftrightarrow |3\rangle$ and $|2\rangle \leftrightarrow |4\rangle$ transitions, respectively. When microwave field ω_3 is added to drive the $|1\rangle \leftrightarrow |4\rangle$ transition, such a system is equivalent to our four-level atom with SGC in the dressed state representation.

Another possibility is to use a four-level inverted-Y configuration in an asymmetric QW. By choosing the materials and structure dimensions in device design, we can have the proper parametric conditions. The system considered here

is similar to the ones used in Refs. [51]–[54] as shown in Figs. 10(b) and 10(c). A weak probe field ω_p is applied to the transition $|1\rangle \leftrightarrow |2\rangle$, while the transitions $|2\rangle \leftrightarrow |3\rangle$ and $|2\rangle \leftrightarrow |4\rangle$ are mediated by coupling fields ω_1 and ω_2, respectively. The cycling field ω_3 is coupled to the transition $|1\rangle \leftrightarrow |4\rangle$ to simulate the SGC. In the dressed state representation, such a QW system is also equivalent to our four-level atom with SGC. So it can be expected that various effects of the SGC on the gain properties should be possibly demonstrated in semiconductor QWs experimentally.

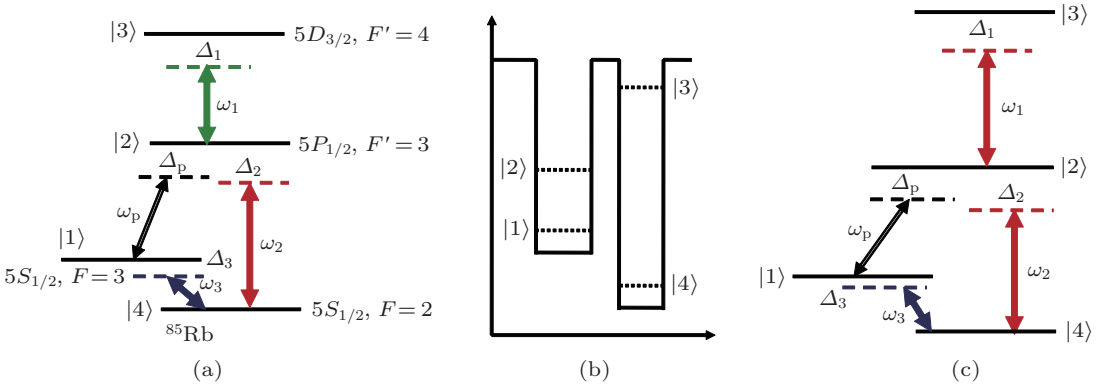

Fig. 10. (color online) Energy-level schemes for (a) ^{85}Rb, (b) the four-level inverted-Y quantum well system, and (c) the QW system.

6. Conclusion

In this paper, we investigated the effects of SGC on the steady and transient gain properties in a four-level inverted-Y-type system. For the steady process, the inversionless gain can be achieved due to the SGC effect as well as the DIC effect, but the former contributes more to the inversionless gain. In particular, the inversionless gain becomes quite sensitive to the relative phase between the probe and the coupling field. We can modulate the gain profile and the gain amplitude simultaneously by changing the relative phase. Different from the case in the Λ-type atomic system, the amplitude of the probe gain can be much larger and more gain peaks can be obtained in the steady-state response by changing the detuning of the additional coupling field. While for the transient process, we show that the transient gain properties can be greatly affected by the SGC. The behavior of the gain in the transient process is also very sensitive to the relative phase between the probe and the coherent field. Transient gain can be dramatically enhanced due to the effect of SGC, and the transient absorption can be completely eliminated by choosing a proper relative phase. Finally, we discuss possible experiments in which these results, in both atomic and QW systems, can be achieved.

References

[1] Scully M O, Zhu S Y and Gavrielides A 1989 *Phys. Rev. Lett.* **62** 2813
[2] Imamoglu A, Field J E and Harris S E 1991 *Phys. Rev. Lett.* **66** 1154
[3] Harris S E 1989 *Phys. Rev. Lett.* **62** 1033
[4] Harris S E and Macklin J J 1989 *Phys. Rev. A* **40** 4135
[5] Gao J Y, Guo C, Guo X Z, Jin G X, Wang P W, Zhao J, Zhang H Z, Jiang Y, Wang D Z and Jiang D M 1992 *Opt. Commun.* **93** 323
[6] Zibrov A S, Lukin M D, Nikonov D E, Hollberg L, Scully M O, Velichansky V L and Robinson H G 1995 *Phys. Rev. Lett.* **75** 1499.
[7] Padmabandu G G, Welch G R, Shubin I N, Fry E S, Nikonov D E, Lukin M D, and Scully M O 1996 *Phys. Rev. Lett.* **76** 2053
[8] Mompart J and Corbalan R 2000 *J. Opt. B: Quantum Semiclass. Opt.* **2** R7
[9] Wu H B, Xiao M and Gea-Banacloche J 2008 *Phys. Rev. A* **78** 041802(R)
[10] Kilin S Y, Kapale K T and Scully M O 2008 *Phys. Rev. Lett.* **100** 173601
[11] Scully M O 2010 *Phys. Rev. Lett.* **104** 207701
[12] Dorfman K E, Jha P K and Das S 2011 *Phys. Rev. A* **84** 053803
[13] Frogley M D, Dynes J F, Beck M, Faist J and Philips C C 2006 *Nat. Mater.* **5** 175
[14] Zhou P and Swain S 1997 *Phys. Rev. Lett.* **78** 832
[15] Agarwal G S 1974 *Quamtum Optics: Springer Tracts in Modern Physics*, Vol. **70** (Berlin: Spriger-Verlag)
[16] Zhu S Y and Scully M O 1996 *Phys. Rev. Lett.* **76** 388
[17] Zhou P and Swain S 1996 *Phys. Rev. Lett.* **77** 3995
[18] Paspalakis E, Kylstra N J and Knight P L 1999 *Phys. Rev. Lett.* **82** 2079
[19] Tang Z H, Li G X and Ficek Z 2010 *Phys. Rev. A* **82** 063837
[20] Bennet C H and Divincenzo D P 2000 *Nature* **404** 247
[21] Bajcsy M, Hofferberth S, Balic V, Peyronel T, Hafezi M, Zibrov A S, Vuletic V and Lukin M D 2009 *Phys. Rev. Lett.* **102** 203902
[22] Postavaru O, Harman Z and Keitel C H 2011 *Phys. Rev. Lett.* **106** 033001
[23] Menon S and Agarwal G S 1998 *Phys. Rev. A* **57** 4014
[24] Menon S and Agarwal G S 1999 *Phys. Rev. A* **61** 013807
[25] Dutta S and Dastidar K R 2006 *J. Phys. B: At. Mol. Opt. Phys.* **39** 4525
[26] Cui N, Fan X J, Li A Y, Liu C P, Gong S Q and Xu Z Z 2007 *Chin. Phys.* **16** 718
[27] Wu J H and Gao J Y 2002 *Phys. Rev. A* **65** 063807
[28] Bai Y F, Guo H, Sun H, Han D G, Liu C and Chen X Z 2004 *Phys. Rev. A* **69** 043814
[29] Wu J H, Zhang H F and Gao J Y 2003 *Opt. Lett.* **28** 654
[30] Hou B P, Wang S J, Yu W L and Sun W L 2004 *Phys. Rev. A* **69** 053805
[31] Hou B P, Wang S J, Yu W L and Sun W L 2006 *J. Phys. B: At. Mol. Opt. Phys.* **39** 2335
[32] Xu W H, Wu J H and Gao J Y 2007 *Chin. Phys.* **16** 441
[33] Fan X J, Liu Z B, Liang Y, Jia K N and Tong D M 2011 *Phys. Rev. A* **83** 043805
[34] Xu W H, Wu J H and Gao J Y 2002 *Phys. Rev. A* **66** 063812
[35] Sahrai M and Mahmoudi M 2009 *J. Phys. B: At. Mol. Opt. Phys.* **42** 235503

[36] Fan X J, Liang B, Wang Z D and Tong D M 2010 *Opt. Commun.* **283** 1810
[37] Dawes A M C, Illing L, Clark S M and Gauthier D J 2005 *Science* **308** 672
[38] Yan M, Rickey E G and Zhu Y F 2001 *Phys. Rev. A* **64** 043807
[39] Joshi A and Xiao M 2003 *Phys. Lett. A* **317** 370
[40] Joshi A and Xiao M 2005 *Phys. Rev. A* **71** 041801(R)
[41] Joshi A and Xiao M 2006 *Phys. Rev. A* **74** 052318
[42] Wen J M, Du S W, Zhang Y P, Xiao M and Rubin M H 2008 *Phys. Rev. A* **77** 033816
[43] Kou J, Wan R G, Kang Z H, Wang H H, Jiang L, Zhang X J, Jiang Y and Gao J Y 2010 *J. Opt. Soc. Am. B* **27** 2035
[44] Imamoğlu A 1989 *Phys. Rev. A* **40** 2835
[45] Xia H R, Ye C Y and Zhu S Y 1996 *Phys. Rev. Lett.* **77** 1032
[46] Li L, Wang X, Yang J, Lazarov G, Qi J and Lyyra A M 2000 *Phys. Rev. Lett.* **84** 4016
[47] Ficek Z and Swain S 2004 *Phys. Rev. A* **69** 023401
[48] Wu J H, Li A J, Ding Y, Zhao Y C and Gao J Y 2005 *Phys. Rev. A* **72** 023802
[49] Wang C L, Li A J, Zhou X Y, Kang Z H, Jiang Y and Gao J Y 2008 *Opt. Lett.* **33** 687
[50] Tian S C, Wang C L, Tong C Z, Wang L J, Wang H H, Yang X B, Kang Z H and Gao J Y 2012 *Opt. Express* **20** 23559
[51] Joshi A 2009 *Phys. Rev. B* **79** 115315
[52] Osman K I, Hassan S S and Joshi A 2009 *Eur. Phys. J. D* **54** 119
[53] Wang Z P, Yu B L, Xu F, Zhen S L, Wu X Q, Zhu J and Cao Z G 2012 *Physica E* **44** 1267
[54] Fan S L, Shi Y P, Zhang H J and Sun H 2012 *Chin. Phys. B* **21** 114203